Thermal conductivity of sputtered oxide films

S.-M. Lee and David G. Cahill
Materials Research Laboratory and the Department of Materials Science and Engineering, University of Illinois, Urbana, Illinois 61801

Thomas H. Allen
Optical Coatings Laboratory Inc., Santa Rosa, California 95407-7397
(Received 30 December 1994; revised manuscript received 16 March 1995)

The thermal conductivity of oxide thin films deposited using dc, rf, and ion-beam sputtering is measured in the temperature range 80–400 K using the 3ω method. Thermal conductivity data for amorphous thin films of SiO_2 are nearly identical to bulk a-SiO_2. Data for amorphous Al_2O_3, while having a magnitude and temperature dependence similar to bulk amorphous oxides, show a dependence on deposition method; rf sputtering of an Al_2O_3 target produces films with a thermal conductivity 35% smaller than films prepared by ion-beam sputtering. Microcrystalline thin films show a rich variety of behavior: the conductivity of TiO_2 films depends on the substrate temperature T_s and approaches the thermal conductivity of bulk TiO_2 ceramics when $T_s \simeq 400\,^{\circ}C$; HfO_2 films show glasslike thermal conductivity independent of annealing temperature up to 900 °C; and MgO films display a crystalline thermal conductivity that is greatly reduced relative bulk values.

I. INTRODUCTION

Thin film materials are typically deposited under highly nonequilibrium conditions that lead to microstructures unobtainable in bulk form. The large parameter space of deposition method, substrate temperature, and the composition and pressure of gases used in sputtering processes can be manipulated to control microstructural disorder and therefore properties.[1] In this paper, we describe our study of the the thermal conductivity of oxide thin films deposited using a variety of sputtering processes and explore the range of heat transport behavior displayed by these highly disordered materials.

Our results also have technological relevance to understanding the performance of thermal barrier coatings, optical coatings for high power lasers, magneto-optic storage devices, and microelectronic circuits. Data for the thermal conductivity of oxide films often show large variation between different investigators,[2–7] demonstrating the difficulty in obtaining reliable data for thin films and frustrating efforts to understand and control heat transport in these materials. We anticipate that the data described below will facilitate efforts in applied science aimed, for example, at reducing the thermal conductivity of ceramic coatings used in gas turbine engines[8] and increasing the laser damage threshold of dielectric mirrors and antireflection coatings.[9,10]

II. EXPERIMENTAL DETAILS

Both rf and dc magnetron sputtering were used at the University of Illinois (UI) to prepare thermal conductivity samples, see Table I. During rf magnetron sputter-

TABLE I. Deposition parameters and physical properties of sputtered films. Measurement methods for grain size and density are described in the text; we measure refractive index by ellipsometry. Data for fused quartz, γ-alumina, rutile, MgO and monoclinic HfO_2 are shown in parentheses; data for monoclinic HfO_2 is from Ref. 23; other crystalline densities are from Ref. 29; the others are from Ref. 30. Films are deposited by rf magnetron (rf), dc magnetron (dc) or ion-beam sputtering (IBS). Films are deposited at two sites: University of Illinois (UI) and Optical Coatings Laboratory, Inc. (OCLI). Film thicknesses are in the range 0.5–2.0 μm.

Composition	Average grain size (Å)	Refractive index	Density (g cm^{-3})	Target	Method/Site
SiO_2	Amorphous	1.51(1.46)	2.10(2.20)	a-SiO_2	rf/UI
	Amorphous	1.53	2.20	Si	dc/OCLI
Al_2O_3	Amorphous	1.57–1.7(1.7)	3.40(3.65)	α-Al_2O_3	rf/UI
	Amorphous	1.67	3.51	Al	dc/OCLI
TiO_2	70–170	2.4–2.6(2.76)	4.13(4.26)	Ti	rf/UI
	40	2.1		Ti	IBS/OCLI
	Amorphous	2.01	3.90	Ti	IBS/OCLI
MgO	30–70	1.7–1.75(1.74)	3.50(3.58)	Mg	dc/UI
HfO_2	150	2.04(2.00)	9.1(10.1)	Hf	dc/OCLI

0163-1829/95/52(1)/253(5)/$06.00

ing, the total pressure of the O_2/Ar gas mixture is 5–7×10^{-3} Torr. We deposited films of SiO_2 and Al_2O_3 by rf sputtering of oxide targets; an oxygen partial pressure of 2×10^{-4} Torr is added to avoid oxygen deficiency.[11] For reactive rf sputtering of TiO_2 films from a Ti metal target, we used an O_2 partial pressure of 1.5×10^{-3} Torr. The deposition rate using our rf sputtering system is 0.2–0.5 Å sec^{-1}. MgO films are deposited by dc magnetron sputtering of a Mg metal target. The total gas pressure of the O_2/Ar mixture is fixed at 5×10^{-3} Torr and the oxygen partial pressure is adjusted to the lowest value that maintains an oxygen "covered" target.[12] The deposition rate for MgO films is 1.5 Å sec^{-1}. At Optical Coatings Laboratory (OCLI), we deposited oxide films using ion-beam sputtering and dc reactive magnetron sputtering of metal targets in a reactive atmosphere, see Table I.

Substrate temperatures are not measured directly: for SiO_2 and Al_2O_3 films deposited at UI and all films deposited at OCLI, the substrate is unheated and we estimate the substrate temperature as 100 °C. TiO_2 and MgO films were deposited at UI on heated substrates; the substrate temperatures discussed below are estimated by adding 50 °C to the temperature of the heated substrate holder. All substrate temperatures should be considered approximate and accurate to only ±30 °C.

We determine the density of films prepared at UI by depositing a test film on a glass coverslip placed next to the thermal conductivity sample. Using a microbalance, the mass of the film is measured to ±10 μg and film thickness is measured using ellipsometry (Gaertner model L116C) and profilometry (Dektak model 3030). The accuracy of the density measurement for fixed film thickness depends on the film density: for SiO_2, with a bulk density of 2.1 g cm^{-3}, the precision of our density measurements is ±5% but for the other oxides the precision improves and is limited only by the determination of film thickness, ±2.5%. The density of films deposited at OCLI are characterized by a combination of Rutherford backscattering spectroscopy to measure areal density and profilometry to measure film thickness. The precision of these measurements is estimated at ±3%. The film densities range from 0–6 % lower than bulk densities. (For Al_2O_3, since bulk amorphous Al_2O_3 does not exist, we compare the film density to the lowest density crystalline phase, γ-Al_2O_3.)

X-ray diffraction data show that our sputtered SiO_2 and Al_2O_3 films are amorphous and HfO_2, MgO and all but one of the TiO_2 films are microcrystalline, see Table I. For microcrystalline films, we estimate the average grain size D from the Laue integral width B using the Scherrer equation[13]

$$D = k\frac{\lambda}{(B-b)\cos(\theta)}, \tag{1}$$

where k is the Scherrer constant (we set $k = 1$), λ is the x-ray wavelength, 2θ is the diffraction angle of the peak, and b is the instrumental broadening. For our films, $b/B < 0.15$. The average grain sizes D are summarized in Table I and range from 30 to 200 Å. The grain sizes of TiO_2 films depend on deposition temperature and are discussed more completely below.

Thermal conductivity data are measured by a recently developed extension of the 3ω method.[14] This technique enables the measurement of thin films as thin as 2000 Å when deposited on high thermal conductivity substrates. To prepare a sample for the measurement, a 3000 Å thick Au film is deposited on top of the oxide film with a thin Cr layer for adhesion. The metal film is subsequently patterned into 5 mm × 25 μm line that serves simultaneously as a heater and thermometer. Since the heater width is much larger than the film thickness, 0.5–2.0 μm and the substrate has much higher thermal conductivity than the films, the thermal response of the heater is the superposition of the substrate response and the frequency-independent thermal resistance of the oxide film. For thermal wavelengths smaller than the substrate thickness but much larger than the oxide film thickness, the substrate response is calculable.[15] The thermal conductivity of the films on Si or MgO is measured from the calculated substrate response. At each temperature, data are acquired in the region of 10 Hz–10 kHz. AlN substrate, on the other hand, has such a large thermal diffusivity below 200 K that the thermal wavelength is not confined to the substrate in this frequency region. In this case, we separately measure the thermal response of the bare AlN substrate. By subtracting the response of the substrate from the measured thermal response of the metal line, the thermal resistance of the sample film is measured in the direction perpendicular to the plane of the film.

We have previously demonstrated that a-SiO_2 grown thermally on a Si wafer has a thermal conductivity identical to bulk a-SiO_2 and therefore confirmed the accuracy of our method.[14] Okuda and Ohkubo[5] and Goodson *et al.*[6] have also recently shown that the thermal conductivity of thermal a-SiO_2 near room temperature is comparable to the bulk value.

III. RESULTS AND DISCUSSION

Thermal conductivity data for SiO_2 films deposited by dc and rf sputtering are presented in Fig. 1. We observe little dependence of the data on deposition method or choice of substrate. In addition, the data are reduced by less than 20% from data for thermally grown a-SiO_2 or equivalently bulk a-SiO_2. We can conclude that heat transport in sputtered a-SiO_2 thin films is essentially identical to that of bulk SiO_2 glass.

In Fig. 1, the data are also compared to the minimum thermal conductivity Λ_{min} calculated by assuming that heat is transported by a random walk of vibrational energy between oscillators that have a vibrational lifetime of one half the period of oscillation.[16–18] This model successfully describes the thermal conductivity of a wide range of bulk amorphous solids and strongly disordered crystals at $T > 50$ K.[19] An important feature of the minimum thermal conductivity model is the lack of free parameters: Λ_{min} is based on a Debye model and only the sound velocities and atomic density are needed as inputs. Hence we emphasize that the calculated Λ_{min} is not the

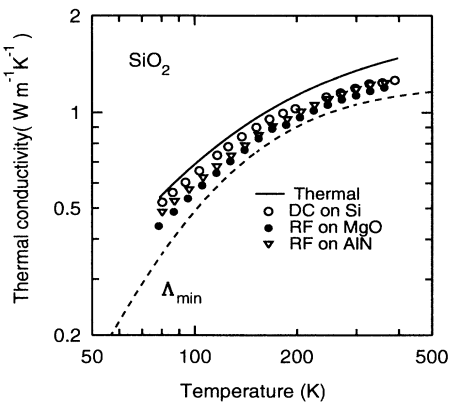

FIG. 1. Thermal conductivity of SiO_2 films. Data for the film thermally grown on Si is nearly equivalent to that of bulk a-SiO_2 (Ref. 14). The data for sputtered films are reduced by less than 20% relative to bulk values and show little dependence on deposition method or choice of substrate. The calculated minimum thermal conductivity Λ_{min} is shown for comparison.

rigorous minimum but rather an estimate of the lowest possible thermal conductivity for the material. Since we have not determined the elastic constants of our thin-film samples, we use elastic constants of bulk phases to calculate Λ_{min}: for SiO_2, see Ref. 20; Al_2O_3, see Ref. 21; TiO_2 and MgO, see Ref. 22; HfO_2, see Ref. 23.

Figure 2 shows that the behavior of Al_2O_3 films is similar to a-SiO_2. As expected for an amorphous solid,[18] the data decrease with decreasing temperature and agree reasonably with the calculated Λ_{min}. Since Al_2O_3 does not have a bulk amorphous phase, we calculate the minimum thermal conductivity using the elastic constants of an α-alumina ceramic with a density of 3.6 g cm^{-3}.[21] Since Λ_{min} is calculated based on a simple model using parameters for α-alumina, it is not unreasonable that the data for rf sputtered films fall somewhat below the calculated

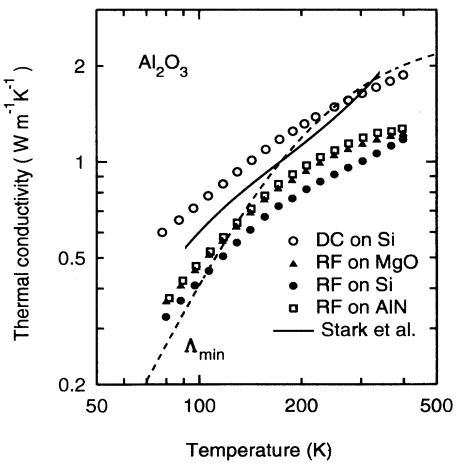

FIG. 2. Thermal conductivity of Al_2O_3 films. Data for film deposited by dc sputtering at OCLI (open circles) are larger than data for rf films deposited at UI by $\sim$ 35%. Data for a free-standing Al_2O_3 film, see (Ref. 24), and the calculated Λ_{min} is shown for comparison.

Λ_{min}. Our data for sputtered films are also comparable to data for a free-standing 140 nm thick film of a-Al_2O_3 prepared using anodic oxidation.[24]

Data for SiO_2 films show little variation with deposition method. Data for Al_2O_3 films, on the other hand, show a significant difference between films deposited by rf and dc sputtering. The density of the dc sputtered film is only a few percent greater than the rf sputtered films but the difference in the thermal conductivity is $\sim$ 35%. (For both rf and dc sputtered films, the film densities are smaller than bulk α-Al_2O_3 and comparable to that of γ-Al_2O_3.) This reduction in thermal conductivity is too large to be easily explained by a small volume fraction of voids[25] and we do not yet understand the origin of this difference between our dc and rf sputtered films.

With one exception, our sputtered TiO_2 films are microcrystalline and have the rutile structure.[26] The thermal conductivity shows a dramatic dependence on substrate temperature, see Fig. 3, and approaches bulk crystalline values for films deposited at 400 °C. Within the precision of our measurements, the film density of 4.1 g cm^{-3} (which is nearly equal to to the density of rutile

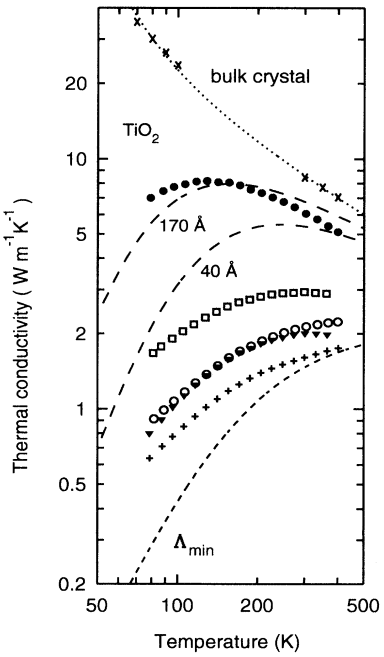

FIG. 3. Thermal conductivity of TiO_2 films. The filled circles and open squares show data for films deposited at 400 and 250°C, respectively. The open circles and filled triangles are data for OCLI and UI films deposited at 100 °C. The data marked by plus signs were obtained on an amorphous sample that was studied in an earlier investigation (Ref. 25). The X symbols indicate recommended values (Ref. 28) for TiO_2 single crystals with heat flow parallel to the c axis (below 100 K) and for TiO_2 ceramics (above 300 K). The dotted line is a Debye model fit to the recommended data. Dashed lines labeled 170 and 40 Å are calculated thermal conductivities using anharmonic phonon-scattering rates determined from a fit to data for the bulk crystal and an additional frequency-independent scattering length of 170 and 40 Å, respectively.

4.26 g cm^{-3}) is independent of substrate temperature. We could, however, observe significant changes in the average grain size measured by x-ray diffraction, see Figs. 3 and 4.

The grain size alone, however, is insufficient to explain the dependence of the data on substrate temperature. In addition to the data shown in Fig. 3, we also plot a calculation of the expected thermal conductivity using a Debye model[27] with anharmonic phonon-scattering rates determined from a fit to data for bulk TiO_2.[28] Including a grain boundary scattering term with a wavelength-independent mean free path of 170 Å, we tried to fit data for the sample deposited at 400 °C. Decreasing the boundary scattering length to 40 Å produces the dashed line. We see that boundary scattering alone cannot explain the greatly reduced thermal conductivity of samples deposited near room temperature. We believe that atomic-scale defects frozen in during deposition result in enough disorder to produce a glasslike thermal conductivity. Glasslike thermal conductivities are observed in a number of strongly disordered bulk crystalline solids that contain large concentration of interstitials or vacancies.[19] Increasing the substrate temperature increases the grain size but, more importantly, decreases the density of the atomic-scale defects.

In Fig. 4 we plot the thermal conductivity at two temperatures as a function of grain size to emphasize our point that grain boundary scattering is too weak to explain the glasslike thermal conductivity of films deposited near room temperature. The calculated thermal conductivity is only weakly dependent on grain size D, while the experimental data decrease abruptly near $D = 100$ Å.

Similarly, grain-boundary scattering cannot explain the glasslike thermal conductivity we observe in microcrystalline, monoclinic HfO_2, see Fig. 5. While the average grain size is 150 Å, comparable to the grain size of our highest thermal conductivity TiO_2 film, data for HfO_2 decrease with decreasing temperature and are comparable to the calculated minimum thermal conductivity. The density of HfO_2 film, 9.1 g cm^3, is < 90% of the crystalline density and high-temperature annealing of the film enhances its thermal conductivity by less than 20%. The thermal conductivity for this single component and microcrystalline film resembles that of related bulk material, the mixed crystal stabilized zirconia.[19] A large concentration of oxygen vacancies is thought to create the glasslike thermal conductivity of stabilized zirconia. Again, we speculate that interstitials and vacancies produced during film deposition are responsible for the glasslike thermal conductivity of this microcrystalline oxide thin film.

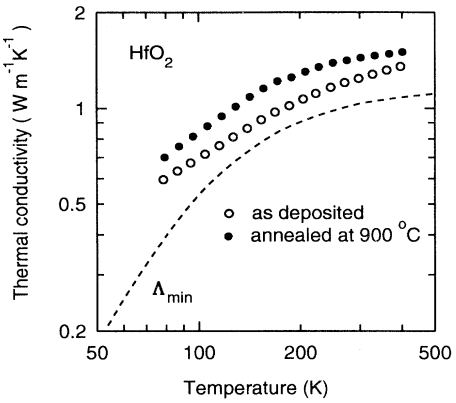

FIG. 5. Thermal conductivity of HfO_2 films. Annealing at 900 °C increases the thermal conductivity by less than 20%. Although the film is microcrystalline with average grain size 150 Å, the thermal conductivity displays a temperature dependence typical of amorphous solids.

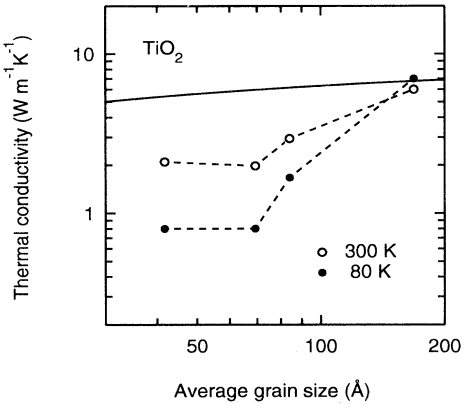

FIG. 4. Plot of the relation between the thermal conductivity and average grain size of the microcrystalline films of TiO_2. The solid and open circles are data taken at 80 and 300 K, respectively. The dashed lines are intended as a guide to the eye. The average grain size are determined from the x-ray diffraction data. The grain size D is a function of the deposition temperature T_s: at $T_s = 400$ °C, $D = 170$ Å, at $T_s = 250$ °C, $D = 85$ Å, at $T_s = 100$ °C, $D = 70$ Å for the rf sputtered film and $D = 40$ Å for the dc sputtered film. The solid line is the calculated thermal conductivity at 300 K.

In contrast to the strong dependence on deposition temperature we observe for TiO_2, Fig. 6 shows that data

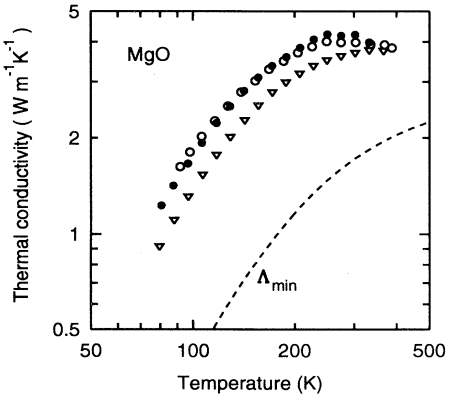

FIG. 6. Thermal conductivity of MgO films. Open circles, solid circles, and open triangles are data for films deposited at 100, 250, and 400 °C, respectively. The data exceed the calculated minimum Λ_{min} by roughly a factor of 3 and show a weak maximum near room temperature that is characteristic of crystalline thermal conductivity behavior.

for MgO films are nearly independent of substrate temperature. The MgO films have an average grain size of 30–70 Å and the data exceed the calculated minimum by roughly a factor of 3. The data also show a weak maximum near room temperature that is characteristic of crystalline thermal conductivity behavior[18] but we note that the room-temperature value is approximately a factor of 10 smaller than data for single-crystal MgO. The density of point defects in our MgO films is apparently small enough so that the thermal conductivity is more typical of a moderately disordered crystal than of the glasslike thermal conductivity of a strongly disordered crystal.[19]

We have listed the densities of the films as well as their bulk densities in the Table I. The density of microcrystalline TiO_2 and MgO films are above 97% of their crystalline density and they show crystalline thermal conductivity. HfO_2 film, on the other hand, has density about 90% of the crystalline density and shows glasslike thermal conductivity. We may deduce that the thermal conductivity of microcrystalline films is related to the film density as well as the grain size. This contrasts with the results for amorphous films. Although the amorphous films of SiO_2, Al_2O_3, and TiO_2 have densities ranging 80–96 % of the crystalline density and data of Al_2O_3 films indicate noticeable density dependence, all of them have glasslike thermal conductivity which is about the calculated thermal conductivity minimum.

IV. CONCLUSION

A wide variety of behavior is observed in the thermal conductivity of sputtered oxide thin films. But we emphasize that the general features of the thermal conductivity can be understood on the basis of the known behavior of bulk glasses and strongly disordered crystals. The thermal conductivity of amorphous thin films, for example SiO_2 and Al_2O_3, are comparable to what is expected for bulk amorphous oxides. The thermal conductivity of microcrystalline thin films, as exemplified by TiO_2, can span the range from the low glasslike thermal conductivity expected for heavily disordered crystals to the high thermal conductivities characteristic of bulk crystals.

ACKNOWLEDGMENTS

This work was supported by the U.S. Department of Energy Grant No. DEFG02-91-ER45439 through the University of Illinois Materials Research Laboratory. Sample characterization was carried out in the Center for Microanalysis of Materials, University of Illinois, which is supported by the U.S. Department of Energy under Grant No. DEFG02-91-ER45439. We also thank the Korea Science and Engineering Foundation (KOSEF) for financial support.

[1] J. E. Greene, in *Handbook of Crystal Growth* (Elsevier Science, Amsterdam, 1993), p. 641.
[2] D. Ristau and J. Ebert, Appl. Opt. **25**, 4571 (1986).
[3] J. C. Lambropoulos, M. R. Jolly, C. A. Amsden, S. E. Gilman, M. J. Sinicropi, D. Diakomihalis, and S. D. Jacobs, J. Appl. Phys. **66**, 4230 (1989).
[4] C. H. Henager, Jr. and W. T. Pawlewicz, Appl. Opt. **32**, 91 (1993).
[5] M. Okuda and S. Ohkubo, Thin Solid Films **213**, 176 (1992).
[6] K. E. Goodson, M. I. Flik, L. T. Su, and D. A. Antoniadis, IEEE Trans. Electron Devices Lett. **14**, 490 (1993).
[7] Z. L. Wu, M. Reiching, X.-Q. Hu, K. Balasubramanian, and K. H. Guenther, Appl. Opt. **32**, 5660 (1993).
[8] S. M. Meier and D. K. Gupta, J. Eng. Gas Turbines Power **116**, 250 (1994).
[9] A. H. Guenther and J. K. McIver, Thin Solid Films **163**, 203 (1988).
[10] B. S. W. Kuo and A. W. Schmid, J. Appl. Phys. **74**, 5159 (1993).
[11] G. Holmén and H. Jacobsson, J. Appl. Phys. **68**, 2962 (1990).
[12] R. Parsons, in *Thin Film Processes II*, edited by J. L. Vossen and W. Kern (Academic, New York, 1991), p. 191.
[13] L. V. Azàroff, *Elements of X-ray Crystallography*, (McGraw-Hill, New York, 1968), p. 549.
[14] David G. Cahill, M. Katiyar, and J. R. Abelson, Phys. Rev. B **50**, 6077 (1994).
[15] David G. Cahill, Rev. Sci. Instrum. **61**, 802 (1990).
[16] A. Einstein, Ann. Phys. **35**, 679 (1911).
[17] G. A. Slack, in *Solid State Physics: Advances in Research and Applications*, edited by F. Seitz and A. G. Turnball (Academic, New York, 1979), Vol. 34, p. 1; see p. 57.
[18] David G. Cahill and R. O. Pohl, Annu. Rev. Phys. Chem. **39**, 93 (1988).
[19] David G. Cahill, S. K. Watson, and R. O. Pohl, Phys. Rev. B **46**, 6131 (1994).
[20] W. F. Love, Phys. Rev. Lett. **31**, 822 (1973). v_t = 3.7 km sec^{-1} and v_l = 5.8 km sec^{-1}.
[21] *Practical Handbook of Materials Science*, edited by C. T. Lynch (CRC, Boca Raton, 1989), p. 301. v_l = 8.8 km sec^{-1} and v_t is estimated to be 5.74 km sec^{-1}.
[22] G. Simmons and H. Wang, *Single Crystal Elastic Constants and Calculated Aggregate Properties* (MIT, Cambridge, MA, 1971). The spatially averaged speeds of sound in MgO are approximately v_l = 9.6 km sec^{-1} and v_t = 6.0 km sec^{-1}; in TiO_2, v_l = 9.2 km sec^{-1} and v_t = 5.1 km sec^{-1}.
[23] J. Wang, H. P. Li, and R. Stevens, J. Mater. Sci. **27**, 5397 (1992). v_l and v_t are assumed to be 4.8 km sec^{-1} and 3.3 km sec^{-1}.
[24] I. Stark, M. Stordeur, and F. Syrowatka, Thin Solid Films **226**, 185 (1993).
[25] David G. Cahill and T. H. Allen, Appl. Phys. Lett. **65**, 309 (1994).
[26] Anatase structure TiO_2 films were observed by D. Wicaksana, A. Kobayashi, and A. Kinbara, J. Vac. Sci. Technol. **A** 10, 1479 (1992).
[27] Philip. D. Thatcher, Phys. Rev. **156**, 975 (1967).
[28] *Thermophysical Properties of Matter*, edited by Y. S. Touloukian (IFI/Plenum, New York, 1970).
[29] Landolt-Börnstein, New Series, Group III, Vol. 7, pt. b1, edited by K.-H. Hellwege and A.M. Hellwege (Springer-Verlag, Berlin, 1975).
[30] *CRC Handbook of Chemistry and Physics*, 75th ed., edited by David R. Lide (CRC, Boca Raton, 1994).